Statistical Properties of Stimulated Raman Crosstalk in WDM Systems

Keang-Po Ho, *Member, IEEE*

Abstract—The crosstalk variance of stimulated Raman crosstalk in wavelength-division-multiplexing (WDM) systems is derived analytically in a closed-form formula for all systems with different walkoff length. The probability density function (pdf) of stimulated Raman crosstalk is found to be lognormal distribution (Gaussian distribution in decibel scale). Both power penalty and power limit induced by Raman crosstalk are evaluated and can be applied to single- and multispan WDM systems.

Index Terms—Fiber nonlinearities, noise statistics, stimulated Raman scattering (SRS), wavelength-division multiplexing (WDM).

I. INTRODUCTION

OPTICAL networks using wavelength-division-multiplexing (WDM) technology are going to revolutionize broadband networks by fully utilizing the enormous bandwidth in an optical fiber. However, stimulated Raman scattering (SRS) [1]–[10] may limit the performance of a WDM system. SRS in WDM systems induces interchannel modulation between each WDM channel by either power depletion or amplification. The launched power into the system is limited because of these Raman crosstalk effects.

The effects of SRS to WDM systems were first discussed in [1] and [2] for maximum power depletion regardless of fiber dispersion, and [3] with fiber dispersion. The optical power limits were evaluated by the worst-case assumption that all WDM channels are synchronized and transmitted at ONE level simultaneously [2], [5]. When random nature of signal modulation was taking into account, the crosstalk variance is reduced for dispersion-shifted fiber (DSF) without pulse walkoff [6], and for highly dispersive fiber with serious pulse walkoff [9]. While most of the papers [1]–[7], [9], [10] assumed negligible signal cross-coupling, negligible pump depletion and/or constant Raman coupling coefficient for a weak signal power, the evolution of SRS induced power variation was studied in [8] for the general case, but with unmodulated channel.

While simple power depletion or amplification can be equalized using optical filter [9], [11], the crosstalk variance degrades the system performance. Although the crosstalk variance could be evaluated accurately for DSF [6], its evaluation for dispersive fiber depends on the assumption that the number of

equally important adjacent bits of adjacent channels that have appreciable SRS interaction over each fiber span is approximately given by $N_b = L_e/L_W$, where L_e is the effective nonlinear length and L_W is the walkoff length. Although that assumption could provide useful result [9], due to fiber attenuation, it is obvious that the first bit and the last bit within the effective nonlinear length contribute differently to the crosstalk variance. Furthermore, the formulae of [9] are not able to generalize to system with long walkoff length because N_b cannot equal to zero in practical systems. An exact analytical expression is derived here to find the crosstalk variance in either time or frequency domain. The expression can be applied for WDM systems with any walkoff length. Simple formulae are also derived as a good approximation for the crosstalk variance for systems with either very short (high dispersion) or long (low dispersion) walkoff length.

To study the SRS induced performance degradation for a WDM system, the probability density function (pdf) of SRS-induced crosstalk is essential. The pdf was given in [6] and [9], [10] for DSF and dispersive fiber, respectively. The pdf was found approximately Gaussian distribution in decibel scale (lognormal distribution in linear scale, see Appendix A) for DSF [6], no method is provided to find the parameters of the pdf until [9] by the same authors. The lognormal distribution was approximated by Gaussian distribution in [9] for performance evaluation. Being very accurate for dispersive fiber, without an analytical expression, the pdf of [10] requires extensive numerical calculation to evaluate. This paper verifies that the pdf of SRS induced crosstalk is lognormal distribution, or Gaussian distribution in decibel scale. The power penalties due to Raman crosstalk are also evaluated.

The remaining parts of this paper will first derive formulae for crosstalk variance and then study the power penalty induced by Raman crosstalk.

II. CROSSTALK VARIANCE

This section will derive the crosstalk variance first for the simplest case of a two-channel system and then for an N-channel system.

A. Two-Channel Pump and Stakes Waves

For the simplest case of a two-channel system, the propagation of the pump and Stokes waves in terms of optical power is governed by two coupled equations [3], [4], [8]–[10], [12]. Similar to [1]–[7], [9], [10], [12], we assume negligible signal cross-coupling and pump depletion. The evolution of pump power is

given by [3], [10]

$$P_p(z,t) = P_p(0,\tau)\,\exp\left[-\alpha z - K\right.$$
$$\left.\cdot \int_0^z P_s(0,\tau - d_{\mathrm{sp}}z')e^{-\alpha z'}\,dz'\right] \quad (1)$$

where P_p and P_s are the power of the pump and Stokes waves, respectively, α is the fiber attenuation coefficient, $\tau = t - z/v_p$, $d_{\mathrm{sp}} = 1/v_s - 1/v_p$ is the walkoff parameter where v_s and v_p are the group velocity of Stokes and pump waves, respectively, $K = g'\Delta f_{\mathrm{sp}}/2A_{\mathrm{eff}}$ where $g' = dg/df$ represents the slope of the Raman gain profile, Δf_{sp} is the frequency separation of the two channels, A_{eff} is the effective cross-sectional area of the fiber. The Raman gain is also assumed to vary linearly with frequency separation as long as the spectral separation below certain limit [2], [5], [6], [8], [9], [12]. The Raman gain is divided by 2 to account for polarization averaging. In dispersive fiber, $d_{\mathrm{sp}} \approx D\Delta\lambda_{\mathrm{sp}}$, where D is the dispersion coefficient and $\Delta\lambda_{\mathrm{sp}} = \lambda_s - \lambda_p$ is the wavelength separation. The expression of (1) also assumes that fiber dispersion just induces pulse walkoff but no pulse distortion [3], [4], [7], [9], [10], [12]–[14]. If a system is modulated by random binary data, the Stokes wave is

$$P_s(0,t) = \sum_{k=-\infty}^{+\infty} b_k p(t - kT) \quad (2)$$

where $b_k = \{0,1\}$ are random binary data, $p(t)$ is the pulse shape, and T is the bit interval. The walkoff distance is given by

$$L_W = T/|d_{\mathrm{sp}}|. \quad (3)$$

If we consider only when $P_p(0,t)$ is at ONE level, ignore all constant factors, from (1), $P_p(0,t) = e^{-x(z,t)}$ where

$$x(z,t) = \sum_{k=-\infty}^{+\infty} b_k q\left(t - \frac{z}{v_p} - kT\right) \quad (4)$$

and

$$q(t) = K \int_0^z p(t - d_{\mathrm{sp}}z')e^{-\alpha z'}\,dz'. \quad (5)$$

If $p(t)$ is rectangular pulse, see Appendix B, the mean and variance of $x(z,t)$ can be evaluated in either time or frequency domain by

$$\mu_x = \frac{1}{2T}\int_{-\infty}^{\infty} q(t)\,dt = \frac{Q(0)}{2T}, \quad (6)$$

$$\sigma_x^2 = \frac{1}{4T}\int_{-\infty}^{\infty} q^2(t)\,dt = \frac{1}{8\pi T}\int_{-\infty}^{\infty}|Q(\Omega)|^2\,d\Omega \quad (7)$$

where $Q(\Omega)$ is the Fourier transform of $q(t)$. With some calculation similar to that in [7], [13], [14], at the end of a fiber distance of $z = L$, we get

$$\|Q(\Omega)\|^2$$
$$= \frac{K^2|P(\Omega)|^2\left[(1 - e^{-\alpha L})^2 + 4e^{-\alpha L}\sin^2\left(\dfrac{d_{\mathrm{sp}}\Omega L}{2}\right)\right]}{\alpha^2 + (d_{\mathrm{sp}}\Omega)^2}$$
$$(8)$$

where $P(\Omega)$ is the Fourier transform of $p(t)$. From (6)
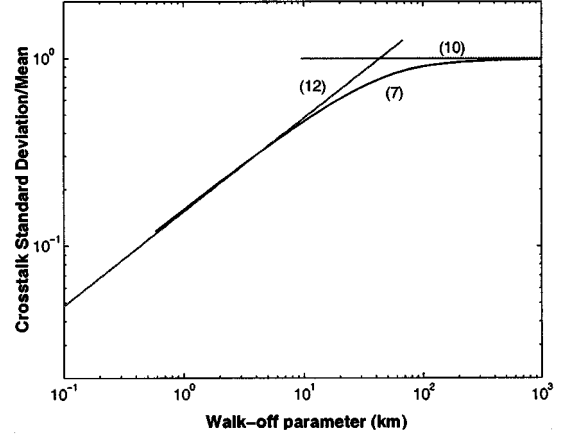
$$\mu_x = KP_0 L_e \quad (9)$$

Fig. 1. The ratio of crosstalk standard deviation to mean σ_x/μ_x as a function of walkoff length L_W. The fiber loss coefficient is $\alpha = 0.2$ dB/km, the fiber distance is $L = 75$ km, and the pump channel is rectangular nonreturn-to-zero (NRZ) pulse stream.

where P_0 is the average launched power and the nonlinear effective length is $L_e = (1 - e^{-\alpha L})/\alpha$.

In some papers [1]–[5], [8], the mean of $x(z,t)$ in (9) may be defined as the power penalty. In practice, the value of $2\mu_x$ is the maximum peak-to-peak Raman crosstalk. With optical filters to equalize the power of all WDM channels, only the variance of $x(z,t)$ is relevant to the performance of the WDM systems.

Without making any physical assumption but simply following some algebra, we have:

Case 1: Walk-off length L_W is very large.

For the example of DSF with large walkoff length L_W

$$\frac{\sigma_x}{\mu_x} = 1 \quad (10)$$

which is the same as [6], [9]. For (10), σ_x is evaluated by using $d_{\mathrm{sp}} = 0$ in (8).

Case 2: Walk-off length L_W is very small.

For a highly dispersive fiber with small L_W (or large d_{sp}) and a long distance fiber having αL larger than unity, $Q(\Omega)$ in (8) is a low-pass signal having 3-dB bandwidth approximately equal to α/d_{sp}. Form Appendix B, for large d_{sp}

$$\sigma_x = KP_0\sqrt{\frac{\alpha L_W}{2}}\,L_e \quad (11)$$

or

$$\frac{\sigma_x}{\mu_x} \approx \sqrt{\frac{\alpha L_W}{2}} \quad (12)$$

which is approximately equal to that of [9] except a factor of $\sqrt{2}$.

Fig. 1 shows the ratio of crosstalk standard deviation σ per channel to crosstalk mean μ_x as a function of walkoff length L_W. In addition to the exact values of (7), Fig. 1 also shows the approximated values given by (10) and (12). The approximation of (12) for short walkoff distance is accurate for L_W less than 10 km. The approximation of (11) is valid for L_W larger than 200 km. Therefore, we may conclude that the model of [6] is precise for L_W larger than 200 km and that of [9] for dispersive fiber, after small modification, is good for L_W less than 10 km.
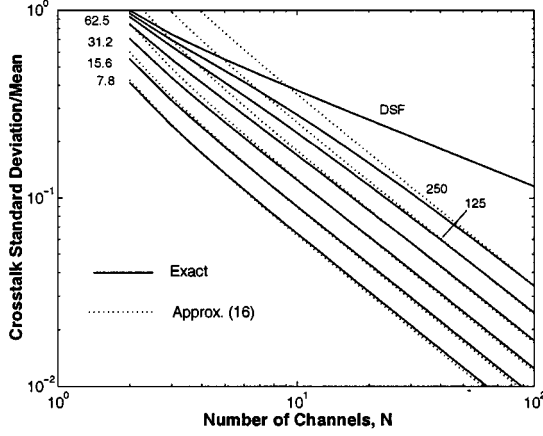
Fig. 2. The ratio of crosstalk standard deviation to mean σ_D/μ_D as a function of number of channels of a WDM system.

Fig. 3. Probability density of SRS induced crosstalk.

The model of [9] for dispersive fiber may not provide a precise estimation for crosstalk variance in some practical systems. For example, the approximation of (12) may not accurate for a 2.5-Gb/s system in standard single-mode fiber (SMF) of $D = 16$ ps/km/nm having $\Delta\lambda < 2.5$ nm, or in nonzero dispersion-shifted fiber (NZDSF) of $D = 4$ ps/km/nm having $\Delta\lambda < 10.0$ nm. However, the approximation of (12) can be used as a worst-case estimation of crosstalk variance. The exact model of (7) is valid for various systems, from highly dispersive to zero-dispersion fiber.

B. N-Channel WDM Systems

In an N-channel WDM system, the channel with the shortest wavelength has the largest power depletion and also the highest crosstalk variance. The overall crosstalk variance, denotes as σ_D^2, can be evaluated by the summation of the crosstalk variance induced by all $N-1$ WDM channels. The walkoff parameter in (8) for the kth adjacent channel is $d_k = kD\Delta\lambda$, where $\Delta\lambda$ is the wavelength separation between adjacent WDM channels. For a multichannel WDM system, without changing the symbol, the walkoff length is defined as

$$L_W = \frac{T}{|D\Delta\lambda|} \tag{13}$$

for the channel separation between adjacent channels.

The overall mean power depletion is given by [1], [2], [5], [6], [9]

$$\mu_D = \frac{N(N-1)}{2} K'P_0L_e \tag{14}$$

where $K' = g'\Delta f/2A_{\text{eff}}$ and Δf is the frequency separation of adjacent WDM channels.

For the extreme cases, we have:

Case 1: Walk-off length L_W is very large.

For the example of DSF with large walkoff length L_W, similar to [9], from Appendix B, we get

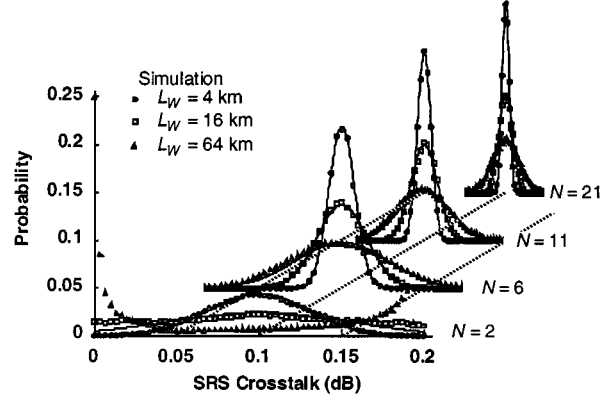$$\frac{\sigma_D}{\mu_D} = \sqrt{\frac{(2(2N-1)}{3N(N-1)}}. \tag{15}$$

Case 2: Walk-off length L_W is very small.

For small L_W, from Appendix B, we get

$$\frac{\sigma_D}{\mu_D} = \sqrt{\frac{\alpha L_W}{N(N-1)}} \tag{16}$$

which is approximately equal to that of [9] in which a factor of 2 was taken into account without detail explanation.

Fig. 2 shows σ_D/μ_D as a function of number of channels of a WDM system, using the exact model and the approximation of (16). The fiber link is the same as that in Fig. 1. The walkoff lengths in Fig. 2 are 250, 125, 62.5, 31.3, 15.6, and 7.8 km. Those walkoff lengths correspond to typical 2.5- and 10-Gb/s WDM systems using SMF or NZDSF, with frequency spacing of $\Delta f = 50$ GHz, 100 GHz, 200 GHz, etc. For examples, the walkoff length of 250 km is for a 2.5-Gb/s WDM system, using NZDSF with $D = 4$ ps/km/nm and channel separation of 0.4 nm (frequency separation of 50 GHz for 1.55 μm system); the walkoff length of 7.8 km corresponds to a 10-Gb/s system, using standard fiber with $D = 16$ ps/km/nm and channel separation of 0.8 nm (frequency separation of 100 GHz).

From Fig. 2, the expression of (16) has no significant difference with the exact model for highly dispersive fiber or when the number of WDM channels increases. The expression of (15) for DSF fiber is a good approximation of fiber with small dispersion and small number of channels, for example, $L_W = 250$ km and $N < 5$.

The accuracy of (16) improves with the increase of dispersion and number of channels. The increase of dispersion and the decrease L_W improves the accuracy of (12) as shown in Fig. 1. When the number of channels increases, the wavelength separation of the farther channels increases. The Raman crosstalk of those farther channels can be predicted by (12) more accurately because of smaller walkoff length. Those farther channels also induce larger Raman crosstalk variance than the closer channels because Raman gain is approximately linearly increase with wavelength separation.

C. Dispersion Compensated Multispan WDM Link

A long-distance fiber communication system usually has many fiber spans. Erbium-doped fiber amplifiers (EDFA) are used in each fiber span to compensate for fiber loss. Usually,
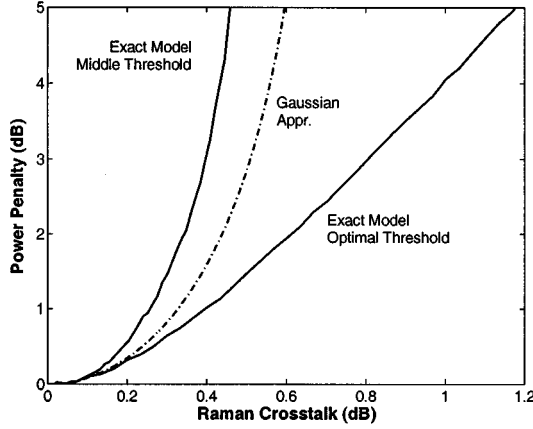
Fig. 4. Raman crosstalk induced power penalty as a function of crosstalk standard deviation σ_0.

each fiber span has the same configuration. The optical power difference due to SRS can be equalized by using optical filters [9], [11]. A multispan fiber link requires dispersion compensation to combat dispersion induced pulse distortion. Dispersion compensator with proper design can induce no fiber nonlinearities to the system, for example, by using low launched power to the dispersion compensation fiber (DCF). While we may extend our model to include SRS in DCF, without loss the insight to the problem, we assume that dispersion compensator induces no SRS.

Like Section II-A, a two-channel pump and Stoke wave system can be considered first. For an M-span fiber system, following the deviation from (1) to (4), at the output of the Mth fiber span, the corresponding expression of (4) is

$$x(ML, t) = \sum_{k=-\infty}^{+\infty} b_k q_M \left(t - \frac{ML}{v_p} - kT \right) \qquad (17)$$

where

$$q_M(t) = \sum_{k=0}^{M-1} q(t - k d_{\mathrm{sp}} \Delta z) \qquad (18)$$

where $q_M(t)$ is the same as that defined in (5), and $d_{\mathrm{sp}} \Delta z = d_{\mathrm{sp}} L + d_c L_c$ is uncompensated pulse walkoff per fiber span, where d_c and L_c are the walkoff parameter and length of the dispersion compensator, respectively. The signs of d_{sp} and d_c are opposite for dispersion compensation. For perfect dispersion compensation, $\Delta z = 0$.

The Fourier transform of $q_M(t)$ is

$$Q_M(\Omega) = Q(\Omega) \sum_{k=0}^{M-1} \exp(-jk\Omega d_{\mathrm{sp}} \Delta z). \qquad (19)$$

The crosstalk variance can be evaluated by substitute (19) to (7). For a bound of the crosstalk variance of (7), we get

$$|Q_M(\Omega)|^2 \le M^2 |Q(\Omega)|^2. \qquad (20)$$

The equality of (20) can be achieved with perfect dispersion compensation of $\Delta z = 0$. We may conclude from (20) that

perfect dispersion compensation is the worst case for crosstalk accumulation. From (7), the crosstalk variance after M spans is

$$\sigma_{x,M} \le M \sigma_x. \qquad (21)$$

Generalized the expressions (17)–(21) to a multichannel WDM system, we may conclude that the crosstalk variance is accumulated span after span in a multispan WDM link with perfect dispersion compensation representing the worst case. With perfect dispersion compensation, the crosstalk variance from an M-span WDM link with launched power of P_0 per span per channel is identical to the crosstalk variance from a single WDM system having launched power of MP_0 per channel.

III. SYSTEM PERFORMANCE

The crosstalk variance in previous section is only one of the parameters for Raman crosstalk. The exact pdf of the Raman crosstalk is required to evaluate the performance degradation.

A. Probability Density Function

From Appendix A, for many random variables multiple together, the pdf of Raman crosstalk can be well approximated by lognormal distribution, especially in highly dispersive fiber or with large number of WDM channels. Lognormal distribution in linear scale is the same as Gaussian distribution in decibel scale. Usually, the summation or multiplication of more than ten independent random variables render the validity of central limit theorem. A simulation is performed to find the required condition to validate the lognormal pdf

Fig. 3 shows the pdf for three walkoff lengths of $L_W = 4, 16,$ and 64 km with $N = 2, 6, 11,$ and 21 WDM channels. The fiber link is identical to that in Fig. 1. The pdf is shown for the worst channel having the smallest wavelength. The average optical power and wavelength separation is chosen such that the mean crosstalk is 0.1 dB, i.e., $\mu_D = 0.1$ dB. The solid curves are the lognormal pdf with parameters given by (14) and Fig. 2. In the region of short walkoff length, for example, $L_W = 4$ km, the pdf is very close to lognormal distribution even for $N = 2$. For all walkoff lengths, the pdf is well approximated by lognormal distribution as the increase of the number of WDM channels. The crosstalk variance decreases as the increase of number of channels.

Using the concept of [9], we may define the number of adjacent bits of adjacent channels that have appreciable SRS interaction is approximately given by $N_b = \max(1, L_e/L_W)$. When the total number of bits from all channels to interact with the channel having the smallest wavelength is larger than 10, the pdf in Fig. 3 can be well approximated by lognormal distribution.

B. System Penalty

Depending on whether the system uses optical filters to equalize the power level, system penalty can be defined differently [9]. In this paper, we always assume that optical filters are used for power equalization.

Raman crosstalk induces waveform distortion when a signal of ONE level is transmitted. Using the lognormal distribution,

$f_Y(y)$, from Appendix A, the bit-error-rate (BER) of a system with Raman crosstalk is

$$p_e = \frac{1}{4} \text{ erfc} \left(\frac{d}{\sqrt{2}\sigma_0} \right) + \frac{1}{4} \int_0^{+\infty} f_Y(y)$$
$$\cdot \text{erfc} \left(\frac{y-d}{\sqrt{2}\sigma_0} \right) \, dy \tag{22}$$

where d is the decision level, σ_0 is the standard deviation of Gaussian noise, and $\text{erfc}(\cdot)$ denotes the complementary error function. The first term of (22) is for BER at ZERO level and the second term is for BER at ONE level. Without Raman crosstalk, with decision level at $d = \mu_y/2$, the system requires $Q_0 = \mu_y/(2\sigma_0) = 6$ to achieve a BER $= 10^{-9}$, where μ_y is the mean optical level at ONE level. With Raman crosstalk, the system requires a larger value of Q_0 for BER $= 10^{-9}$ and $Q_0/6$ can be defined as power penalty.

Depending on the decision circuit, the decision level of (22) can be set at the middle of the eye diagram, i.e., $d = \mu_y/2$, or optimized for minimum BER, i.e., $d = d_{\text{opt}}$. Setting the decision level to zero for an ac-coupled receiver can function as setting the decision level at the middle of the eye diagram. To find the decision level to optimize for minimum BER is more complicated, especially for a time-varying channel requiring adaptation.

Fig. 4 shows the Raman crosstalk induced power penalty as a function of crosstalk standard deviation σ_D. From Appendix A, the crosstalk standard deviation of lognormal distribution is the only relevant parameter for system performance. Fig. 4 also shows the power penalty provided by approximating the lognormal distribution by Gaussian distribution [9], given by[1]

$$-10 \cdot \log_{10}(1 - 36\sigma_D^2) \quad \text{(dB)}. \tag{23}$$

Fig. 4 shows that, at the same level of crosstalk, setting the decision level at the middle of the eye diagram provides the largest power penalty. Because the power penalty of (23) also assumes optimal decision level, from Fig. 4, Gaussian approximation overestimates the power penalty comparing with the exact model of (22) with optimal decision level.

The limitation of the crosstalk standard deviation σ_D may be defined as that for a power penalty of less than 1 dB. The corresponding crosstalk standard deviation is $\sigma_D = 0.25, 0.33,$ and 0.40 dB for the exact model ($d = \mu_y/2$), Gaussian approximation, and exact model ($d = d_{\text{opt}}$). Using more complex decision circuit, optimal decision level can tolerate 60% higher crosstalk level than a middle decision level.

The Gaussian approximation has a fundamental limit of $\sigma_D = 0.72$ dB (1/6 in linear scale) which can be derived obviously from (23) for a power penalty approaching infinity. From Appendix A, the fundamental limit of setting the decision level at the middle of the eye diagram is $\sigma_D = 0.50$ dB.

[1]This power penalty expression is different with that in [9]. Using Gaussian approximation for lognormal distribution, the system Q-factor is

$$Q = \frac{\mu_y}{\sigma_0 + \sqrt{\sigma_0^2 + \sigma_y^2}}$$

and the power penalty for $Q = 6$ can be derived accordingly using (A6) for σ_y.

There is no fundamental limit for the exact model with optimal decision level.

C. System Bounds

Without power equalization, Chraplyvy [5] provides a system bound of

$$N(N-1)P_0\Delta f < 500 \text{ GHz} \cdot \text{W}. \tag{24}$$

Using our symbol, the bound of (24) is for the requirement of $\sigma_D < 1$ dB.

For system with power equalization, with the requirement of $\sigma_D < 0.4$ dB, Fig. 2 can be used to find the power bound of the system. Assuming the following parameters: $T = 400$ ps for a 2.5-Gb/s system, $D = 4$ ps/km/nm for NZDSF, $\Delta\lambda = 0.8$ nm or $\Delta f = 100$ GHz, $N = 64$ as the channel number, the calculation is following:

1) evaluate $L_W = 125$ km, select the corresponding curve in Fig. 2;
2) from $N = 64$, find from Fig. 2 that $\sigma_D/\mu_D = 0.037$;
3) for $\sigma_D < 0.4$ dB, $\mu_D < 10.8$ dB;
4) using the relationship of $N(N-1)P_0\Delta f < 500 \times 10.8$, $P_0 < 11.3$ dBm.

Note that the requirement becomes $MP_0 < 11.3$ dBm for M-span fiber system as from Section II-C. The WDM systems can have no more than 14 fiber spans if the system has a power of 0 dBm per channel, corresponding to a total power of 18 dBm per span.

For the extreme cases, we have

Case 1: Walk-off length L_W is very large.

For the example of DSF with large walkoff length L_W, from (15), after some algebra,

$$\sqrt{N(N-1)(N-1/2)}P_0\Delta f < 173 \text{ GHz} \cdot \text{W}. \tag{25}$$

Case 2: Walk-off length L_W is very small.

For small L_W, after some algebra using (16),

$$\sqrt{(N(N-1)}P_0\Delta f < \frac{200}{\sqrt{\alpha L_W}} \text{ GHz} \cdot \text{W}. \tag{26}$$

The expression of (25) may be valid just for DSF. Depending on number of channels, the validity of (26) may be verified from Fig. 2. In general, the expression of (26) is valid for system using standard fiber with $D = 16$ ps/km/nm and can be used as a worst-case system bound. From the discussion of Section II-C, the bounds of (25) and (26) can also apply to M-span WDM systems by replacing P_0 with MP_0.

IV. CONCLUSION

The probability density function of SRS induced crosstalk is verified to be well approximated by lognormal distribution. When constant gain or loss is equalized, crosstalk ratio, power penalty, and power limit depend only on the crosstalk variance. An exact analytical expression is derived to evaluate the crosstalk variance, valid from highly dispersive to DSF. Using lognormal distribution, power penalty provided by SRS crosstalk is evaluated. The crosstalk standard deviation must be less than 0.4 dB for a power penalty less than 1 dB. With

the requirement of $\sigma_D < 0.4$ dB, power bounds for various system can be found and applied to single- and multispan WDM systems.

APPENDIX A
LOGNORMAL DISTRIBUTION

The lognormal distributed random variable, y, is generated from a Gaussian random variable, x, by the following transformation [15]:

$$y = e^x. \tag{A1}$$

The pdf of lognormal random variable is given by

$$f_Y(y) = \frac{1}{\sqrt{2\pi}\sigma_x y} \exp\left[-\frac{(\ln y - \mu_x)^2}{2\sigma_x^2}\right], \qquad y \geq 0 \tag{A2}$$

where μ_x, σ_x are the mean and standard deviation of the Gaussian random variable x, respectively. The parameter σ_x is called the *shape* parameter of lognormal distribution [15] and σ_x^2 is defined as the crosstalk variance in this paper. It is obvious that a lognormal random variable y is Gaussian distributed in decibel scale. Fig. 3 shows that the simulated pdf approaches lognormal distribution as the increase of channel number or fiber dispersion.

When many independent random variables are added together, the random variable for the summation is Gaussian distributed from the central limit theorem [16]. If many independent random variables multiple together, say $y = \Pi_{k=0}^{N-1} z_k$. It is obvious that $x = \log y = \sum_{k=0}^{N-1} \log z_k$ is Gaussian random variable because it is the summation of many independent random variables. From (A1), y is lognormal distribution. Because Raman crosstalk to a channel from many other WDM channels is the multiplication of the SRS from all bits that interact with the specific channel, the pdf of Raman crosstalk is lognormal distribution.

When a WDM channel is affected by SRS crosstalk, the average optical power is the mean value of $E\{y\}$ given by [15]

$$\mu_y = \exp\left[\mu_x + \frac{\sigma_x^2}{2}\right]. \tag{A3}$$

The variance of a lognormal distributed random variable $E\{(y - \mu_y)^2\}$ is [15]

$$\sigma_y^2 = e^{2\mu_x + \sigma_x^2}[e^{\sigma_x^2} - 1]. \tag{A4}$$

The crosstalk ratio can be defined as the ratio of crosstalk standard deviation to the average optical power:

$$XT = [e^{\sigma_x^2} - 1]^{1/2}. \tag{A5}$$

For small crosstalk of $\sigma_x < 1.3$ dB, $XT = \sigma_x$. The approximation of

$$\sigma_y \approx \sigma_x \mu_y \tag{A6}$$

was used in [9].

If the detection threshold is always at the middle of the eye diagram, i.e., $\mu_y/2$, the probability of error without other noises

is $\Pr\{y < \mu_y/2\}$. After some algebra, for BER less than 10^{-9}, the requirement is

$$\frac{\ln 2 - \sigma_x^2/2}{\sigma_x} > 6 \tag{A7}$$

corresponding to

$$\sigma_x < 0.50 \text{ dB}. \tag{A8}$$

From (A5) and (A8), both crosstalk ratio and fundamental system limits depend only on the shape parameter σ_x. While the pdf is well approximated by lognormal distribution, methods to evaluate σ_x are essential to use the pdf for system performance evaluation.

APPENDIX B
DEVIATION OF CROSSTALK VARIANCE

Here we provide the deviation of some expressions in Section II.

1) Deviation of (6): Ignore the constant time-difference of z/v_p, the crosstalk term of (4) becomes

$$x(t) = \sum_{k=-\infty}^{+\infty} b_k q(t - kT) \tag{B1}$$

that is independent of distance and a cyclostationary random process with period of T. The crosstalk of (B1) is similar to a digital pulse-amplitude modulation (PAM) signal [17]. The mean value of $x(t)$ is

$$\mu_x = \frac{1}{T} \int_0^T \sum_{k=-\infty}^{+\infty} E\{b_k\} q(t - kT) \, dt$$

$$= \frac{1}{2T} \int_0^T \sum_{k=-\infty}^{+\infty} q(t - kT) \, dt \tag{B2}$$

where $E\{b_k\} = 1/2$. Exchanging the integration and summation, we get

$$\mu_x = \frac{1}{2T} \sum_{k=-\infty}^{+\infty} \int_0^T q(t - kT) \, dt$$

$$= \frac{1}{2T} \sum_{k=-\infty}^{+\infty} \int_{-kT}^{-(k-1)T} q(t) \, dt$$

$$= \frac{1}{2T} \int_{-\infty}^{+\infty} q(t) \, dt. \tag{B3}$$

Using properties of Fourier transform, the full expression of (6) can be derived.

2) Deviation of (7): As a cyclostationary process, the variance of $x(t)$ is

$$\sigma_x^2 = \frac{1}{T} \int_0^T E\{x^2(t)\} \, dt - \mu_x^2. \tag{B4}$$

The power spectrum of $x(t)$, from [17], is

$$S_x(\Omega) = \frac{\sigma_b^2}{T} |Q(\Omega)|^2$$

$$+ \frac{2\pi m_b^2}{T^2} \sum_{k=-\infty}^{+\infty} \left|Q\left(\frac{2k\pi}{T}\right)\right|^2 \delta\left(\Omega - \frac{2k\pi}{T}\right) \tag{B5}$$

where $Q(\Omega)$ is the Fourier transform of $q(t)$, $\sigma_b^2 = E\{b_k^2\} - (E(\{b_k\})^2 = 1/4$, and $m_b = E\{b_k\} = 1/2$. Using the relationship of power spectrum and autocorrelation function [17], we get

$$\frac{1}{T}\int_0^T E\{x^2(t)\}\,dt = \frac{1}{2\pi}\int_{-\infty}^{+\infty} S_x(\Omega)\,d\Omega$$
$$= \frac{1}{8\pi T}\int_{-\infty}^{+\infty} |Q(\Omega)|^2\,d\Omega$$
$$+ \frac{1}{4T^2}\sum_{k=-\infty}^{+\infty}\left|Q\left(\frac{2k\pi}{T}\right)\right|^2. \quad (B6)$$

Using (B4) and (6), we get

$$\sigma_x^2 = \frac{1}{8\pi T}\int_{-\infty}^{+\infty}|Q(\Omega)|^2\,d\Omega + \frac{1}{2T^2}\sum_{k=1}^{+\infty}\left|Q\left(\frac{2k\pi}{T}\right)\right|^2. \quad (B7)$$

The expression of (B7) is simplified because $|Q(\Omega)|$ is an even function. If $p(t)$ is nonreturn-to-zero (NRZ) rectangular pulse with $|P(\Omega)|^2 = P_0^2\sin^2(T\Omega/2)/\Omega^2$, from (8), $|Q(2k\pi/T)| = 0$, $k = 1, 2, \ldots$, and the expression of (7) can be derived. The second term of (B7) is usually very small for other nonrectangular pulse shape because $Q(\Omega)$ is a low-pass response.

3) Deviation of (11): If $p(t)$ is a rectangular pulse from 0 to T, at low frequency $|P(\Omega)| = 2P_0T$. From (7), the crosstalk variance is

$$\sigma_x^2 = \frac{1}{8\pi T}\int_{-\infty}^{+\infty}\frac{4K^2P_0^2T^2(1-e^{-\alpha L})^2}{\alpha^2+(d_{\mathrm{sp}}\Omega)^2}\,d\Omega$$
$$= \frac{K^2P_0^2T^2(1-e^{-\alpha L})^2}{2\pi T}\frac{\pi}{\alpha d_{\mathrm{sp}}}. \quad (B8)$$

Using the relationship of (3) and $L_e = (1 - e^{-\alpha L})/\alpha$, the simplification of (B8) gives (11).

4) Deviation of (15) and (16): For long walkoff length of L_W, using (10), we get

$$\sigma_D^2 = \sum_{k=1}^{N-1}\sigma_{x,k}^2 = \sigma_{x,1}^2\sum_{k=1}^{N-1}k^2$$
$$= \sigma_{x,1}^2\frac{N(N-1)(2N-1)}{6} \quad (B9)$$

where $\sigma_{x,k}^2$ is the variance from the kth adjacent channels and $\sigma_{x,1} = \mu_{x,1} = K'P_0L_e$. Using σ_D from (B9) and (13), the expression of (15) can be derived.

For short walkoff length of L_W per channel separation, the walkoff length of kth adjacent channel is L_W/k. Using (11), we get

$$\sigma_D^2 = \sum_{k=1}^{N-1}\sigma_{x,k}^2 = (K'P_0L_e)^2\sum_{k=1}^{N-1}k^2\frac{\alpha L_W}{2k}$$
$$= (K'P_0L_e)^2\frac{\alpha L_W N(N-1)}{4}. \quad (B10)$$

The expression of (16) comes directly from (B10) and (14).

Note that both (B9) and (B10) assume that Raman gain linearly increases with channel separation.

REFERENCES

[1] A. R. Chraplyvy and P. S. Henry, "Performance degradation due to stimulated Raman scattering in wavelength-division-multiplexed optical fiber systems," *Electron. Lett.*, vol. 19, pp. 641–643, 1983.

[2] A. R. Chraplyvy, "Optical power limits in multi-channel wavelength-division-multilplexed systems due to stimulated Raman scattering," *Electron. Lett.*, vol. 20, pp. 58–59, 1984.

[3] D. Cotter and A. M. Hill, "Stimulated Raman crosstalk in optical transmission: Effects of group velocity dispersion," *Electron. Lett.*, vol. 20, pp. 185–187, 1984.

[4] W. Jiang and P. Ye, "Crosstalk in fiber Raman amplification for WDM systems," *J. Lightwave Technol.*, vol. 7, pp. 1407–1411, 1989.

[5] A. R. Chraplyvy, "Limitation on lightwave communications imposed by optical-fiber nonlinearities," *J. Lightwave Technol.*, vol. 8, pp. 1548–1557, 1990.

[6] F. Forghieri, R. W. Tkach, and A. R. Chraplyvy, "Effect of modulation statistics on Raman crosstalk in WDM systems," *IEEE Photon. Technol. Lett.*, vol. 7, pp. 101–103, 1995.

[7] Z. Wang, A. Li, C. J. Mahon, G. Jacobsen, and E. Bodtker, "Performance limitations imposed by stimulated Raman scattering in optical WDM SCM video distribution systems," *IEEE Photon. Technol. Lett.*, vol. 7, pp. 1492–1494, 1995.

[8] D. N. Christodoulides and R. B. Jander, "Evolution of stimulated Raman crosstalk in wavelength division multiplexed sytems," *IEEE Photon. Technol. Lett.*, vol. 8, pp. 1722–1724, 1996.

[9] F. Forghieri, R. W. Tkach, and A. R. Chraplyvy, "Fiber nonlinearities and their impact on transmission systems," *Optical Fiber Telecommunications IIIA*, pp. 196–264, 1997.

[10] J. Wang, X. Sun, and M. Zhang, "Effect of group velocity dispersion on stimulated Raman crosstalk in multichannel transmission systems," *IEEE Photon. Technol. Lett.*, vol. 10, pp. 540–542, 1998.

[11] X. Y. Zou, S. M. Hwang, and A. E. Willner, "Compensation of Raman scattering and EDFA's nonuniform gain in ultra-long-distance WDM links," *IEEE Photon. Technol. Lett.*, vol. 8, pp. 139–141, 1996.

[12] G. P. Agrawal, *Nonlinear Fiber Optics.* San Diego, CA: Academic, 1995, ch. 8.

[13] K.-P. Ho, E. Kong, L. Y. Chan, L.-K. Chen, and F. Tong, "Analysis and measurement of root-mean-squared bandwidth of cross-phase modulation induced spectral broadening," *IEEE Photon. Technol. Lett.*, vol. 11, pp. 1126–1128, Sept. 1999.

[14] T. K. Chiang, N. Kagi, M. E. Marhic, and L. G. Kazovsky, "Cross-phase modulation in fiber links with multiple optical amplifiers and dispersion compensators," *J. Lightwave Technol.*, vol. 14, pp. 249–259, 1996.

[15] E. L. Crow and K. Shimizu, *Lognormal Distributions: Theory and Applications.* New York: Marcel Dekker, 1988, ch. 1.

[16] W. B. Davenport, Jr. and W. Root, *An Introduction to the Theory of Random Signals and Noise.* New York: IEEE Press, 1987, pp. 81–84.

[17] J. G. Proakis and M. Salehi, *Communication Systems Engineering.* Upper Saddle River, NJ: Prentice-Hall, 1994, pp. 537–542.

Keang-Po Ho (S'91–M'95) received the B.S. degree from National Taiwan University, Taipei, Taiwan, China, in 1991 and the M.S. and Ph.D. degrees from the University of California at Berkeley in 1993 and 1995, respectively, all in electrical engineering.

He performed research in IBM T. J. Watson Research Center, Hawthorne, NY, on all-optical networks in the summer of 1994. He was a Research Scientist with Bellcore, currently Telcordia Technologies, Red Bank, NJ, from 1995 to 1997, conducted research on optical networking, high-speed lightwave systems, and broad-band access. He joined the Department of Information Engineering of the Chinese University of Hong Kong (CUHK), China, in 1997. His current interests include optical communication systems, multimedia communication systems, combined source-channel coding, and communication theory. He has published over 100 journal and conference articles in these fields.